EPJ Web of Conferences **86**, 00052 (2015)
DOI: 10.1051/epjconf/20158600052

Fission excitation function for ^{19}F + ^{194,196,198}Pt at near and above barrier energies

Varinderjit Singh,[1,a] B.R. Behera,[1] Maninder Kaur,[1] A. Jhingan,[2] P. Sugathan,[2] Santanu Pal,[3] Davinder Siwal,[2,4] M. Oswal,[1] K.P. Singh,[1] S. Goyal,[4] A. Saxena,[5] and S. Kailas[5]

[1]Department of Physics, Panjab University, Chandigarh 160014, India.
[2]Inter University Accelerator Centre, Aruna Asaf Ali Marg, New Delhi 110067, India.
[3]CS-6/1, Golf Green, Kolkata 700095, India.
[4]Department of Physics and Astrophysics, University of Delhi, Delhi 110007, India.
[5]Nuclear Physics Division, Bhabha Atomic Research Centre, Mumbai 400085, India.

Abstract. Fission excitation functions for ^{19}F + ^{194,196,198}Pt reactions populating ^{213,215,217}Fr compound nuclei are reported. Out of these three compound nuclei, ^{213}Fr is a shell closed (N=126) compound nucleus and the other two are away from the shell closure. From a comparison of the experimental fission cross-sections with the statistical model predictions, it is observed that the fission cross-sections are underestimated by the statistical model predictions using shell corrected finite range rotating liquid drop model (FRLDM) fission barriers. Further the FRLDM fission barriers are reduced to fit the fission cross-sections over the entire measured energy range.

1 Introduction

It is now established that the Kramers' predicted fission width involving nuclear dissipation [1] is necessary to reproduce observables in heavy ion induced fusion-fission reactions. A number of measurements were carried out in the past to estimate the magnitude of nuclear dissipations using neutron multiplicity, charged particle multiplicity, GDR γ-ray multiplicity, fission cross-sections and evaporation residue cross-section as probe. From these studies it is found that dissipation effect comes into play at nuclear temperatures above 1 MeV [2].

The dissipation can influence the capture probability of a projectile by the target and also the de-excitation of the excited compound nucleus (CN). Hence it becomes necessary to understand the nature and magnitude of the dissipation. Most of the studies about the nuclear dissipation are based on the neutron, charged particle and GDR γ-ray multiplicity measurements. These probes are sensitive to the dissipation over the whole path of fission process i.e. from equilibrium to scission and hence cannot distinguish the pre and post-saddle dissipation (deformation dependence of nuclear dissipation). Since the decision whether the CN will undergo fission or will result in the formation of a evaporation residue (ER) is taken at saddle point, the fission and ER cross-sections are sensitive only to the dissipation within the saddle point. Here it must be added that the above statement holds in the absence of non-compound processes (quasi or fast fission). In our investigation based on the neutron multiplicity measurement for ^{19}F + ^{194,196,198}Pt reactions, it has been observed that the non-compound nuclear processes are negligible for these reactions [3]. Hence measurement of fission cross-sections for these reactions can be used to get the information about the pre-saddle dissipation.

Another important aspect addressed in the present study is to understand the effect of shell closure on the survival probability of an ER. With this motivation, the fission-fragment angular distributions (fission cross-section) are measured for ^{19}F + ^{194,196,198}Pt at beam energy range 90-118 MeV (excitation energy (E^*) = 45-72.6 MeV).

2 Experimental Arrangements

The experiment is performed at the General Purpose Scattering Chamber (GPSC). A DC beam of ^{19}F in the energy range of 90.5 to 118.7 MeV delivered by the 15 UD Pelletron at IUAC, New Delhi is made to incident on ^{194}Pt, ^{196}Pt and ^{198}Pt targets of thicknesses ~ 1.75 mg/cm^2. Fission fragments are detected using two different detector setups placed on arms of the scattering chamber on the either side of beam direction. On one arm of scattering chamber, two Si surface barrier telescope (T_1 and T_2 in Fig. 1) detectors (SSBD) are placed at a

[a] Corresponding author: Mangat_phy@yahoo.co.in

distance of 13 cm (collimator size 5 mm) with angular separation of 24°. On the other arm, three hybrid [4] telescope (T_3, T_4 and T_5 in Fig. 1) detectors (ΔE gas detector and E SSBD) are placed at a distance of 28 cm (collimator size 10 mm) with angular separation of 12° between two adjacent detectors. Two SSB detectors are kept at ± 10° with a distance of 70 cm (collimator size 1 mm) for monitoring and normalization purpose. Another monitor detector is placed at 60° at a distance of 29 cm. The trigger for the data acquisition system is generated using the OR of timing signals of the two detector setups along with the monitor detectors.

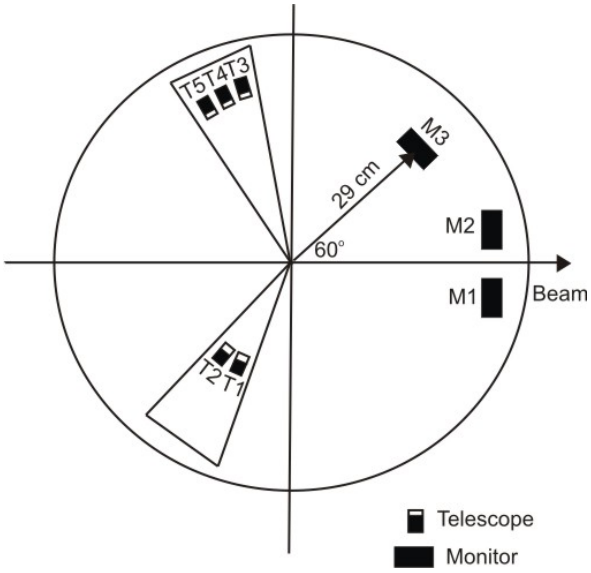

Figure 1. Schematic representation of the experimental setup used for the fission fragments angular distribution measurement. Here T_1 and T_2 are SSBD telescope detectors, T_3, T_4 and T_5 are the hybrid telescope detectors and M_1, M_2 and M_3 are the monitor detectors.

The data from both telescope systems were analyzed independently so that the working of both types of the telescope detectors can be compared. The fission angular distribution data is recorded in the angular range of 78°-168°.

3 Data analysis and results

The measured fission yield of each detectors is normalized using the inter detector normalization and monitor yield. The experimental fission fragment angular distribution is transformed from laboratory to center-of-mass frame using the Viola systematics [5] for symmetric fission. The measured angular distribution is fitted with the theoretical expression for angular distribution of fission fragments given by

$$W(\theta) \propto \sum_{J=0}^{\infty} (2J+1) T_J \frac{\sum_{K=-J}^{J} \frac{1}{2}(2J+1)\,|\,d^J_{0K}(\theta)\,|^2 \exp[\frac{-K^2}{2K_o^2}]}{\sum_{K=-J}^{J} \exp[\frac{-K^2}{2K_o^2}]}$$

where T_J is the transmission coefficient for fusion of J^{th} partial wave and K_o is the standard deviation of the K distribution. In this minimization procedure the K_o is treated as a free parameter. The fitted angular distributions for $^{19}F + ^{196}Pt$ at beam energy of 105.9 MeV for both the telescope detectors is shown in Fig. 2. The yield of fission fragments produced from the compound nucleus is symmetric about 90°. Hence the total fission

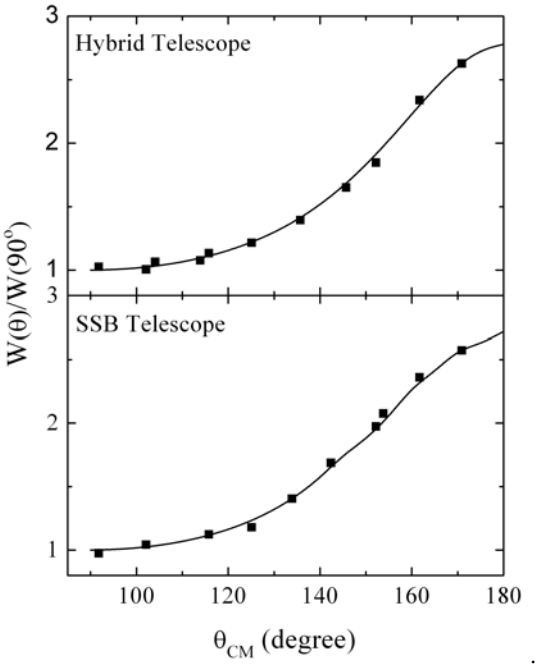

Figure 2. Experimental fission fragments angular distribution (solid square) for $^{19}F + ^{196}Pt$ reaction at 105.9 MeV obtained using both telescope detectors. Solid lines are the angular distributions obtained by fitting the experimental data.

yield from 0° to 180° (say *sum*) is obtained by multiplying the fission yield from 90° to 180° by 2, given as

$$sum = 2\pi \int_{\pi/2}^{\pi} W(\theta_{CM}) \sin(\theta_{CM}) d\theta_{CM}$$

where $W(\theta_{CM})$ is the ratio of fission yield to the monitor yield at an angle θ_{CM} in the center of mass frame. The total fission cross-section is obtained as

$$\sigma_{fiss} = \frac{1}{2} sum \frac{\Omega_{mon}}{\Omega_{fiss}} \sigma_{ruth}$$

where Ω_{fiss} and Ω_{mon} are the solid angles subtended by the fission and the monitor detector respectively and σ_{ruth} is Rutherford cross-section. The fission excitation function for different compound nuclei obtained using both hybrid and SSB telescope detectors setup are shown in Fig. 3 and 4 respectively. The fission cross-section obtained from two different set of telescope detectors are found to be within error bars. It is observed that the fission cross-sections increase as one goes from ^{217}Fr to ^{213}Fr. This observation is in agreement with the expectations based on fissility parameter values. From this observation one

can conclude that the shell closure in CN (^{213}Fr) does not provide any extra stability against fission.

4 Statistical model calculations

The experimentally obtained fission cross-sections are compared with the statistical model predictions. Emission of neutrons, protons, α-particles, giant dipole resonance (GDR) γ-rays and formation of ERs are considered as the possible modes of decay for a compound nucleus. The light particles and the γ-decay widths are obtained from the Weisskopf formula [6]. The fission width is obtained using Bohr-Wheeler formula [7]. The level density parameter is taken from Ignatyuk *et al.* [8] which take into account the nuclear shell structure effect at low excitation energies. The experimental masses have been used to obtain the particle binding energies. The calculations are performed using the shell corrected Finite range Rotating Liquid Drop model (FRLDM) barrier. The shell correction in fission barrier is incorporated using the prescription suggested by Aritomo [9].

Another important ingredient in statistical model is spin distribution. In present investigations the spin distribution has been obtained by fitting the experimental fusion cross-section with coupled channel calculations based code CCDEF [10]. The fusion cross-sections at low energy were measured by Mahata *et al.* [11] whereas the fusion cross-sections at higher energies is obtained by adding fission cross-sections measured in present work with the ER cross-sections measured earlier [12]. The potential parameters are adjusted to fit the experimental cross-sections at energies well above the barrier. The inelastic states of the target are coupled using the vibrational model, calculating the coupling strength from the collective model. The 2^+ and 3^- states of the target are included in the calculations. The quadrupole [13] and hexadecapole [14] deformation of targets are also taken into account. The deformation parameters and corresponding excitation energies of different states for ^{194,196,198}Pt are listed in Table 1.

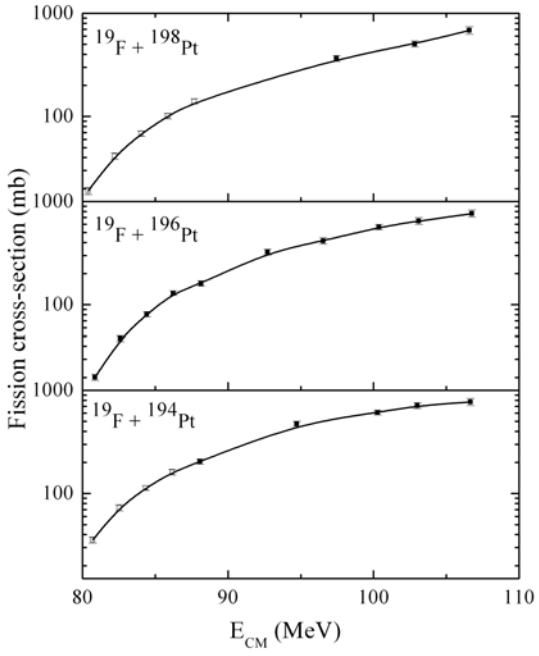

Figure 3. Experimental fission cross-sections for different reactions obtained using Hybrid telescope detectors. The solid squares are the present measurements and open squares are measurements by Mahata *et al.* [11]. Solid line is to guide the eyes.

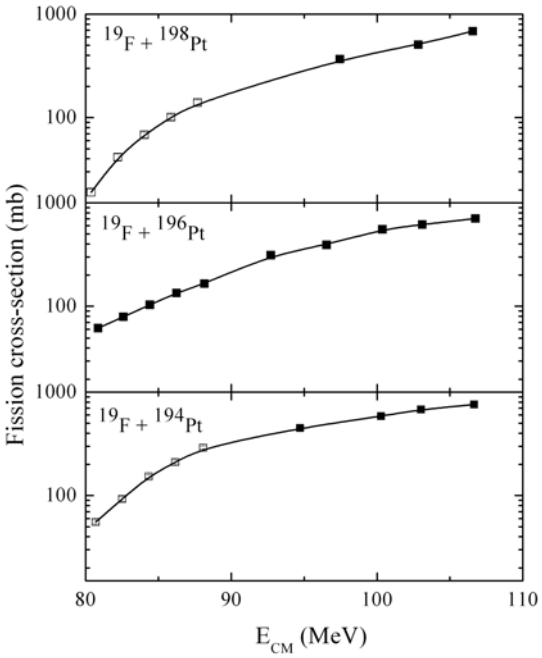

Figure 4. Experimental fission cross-sections for different reactions obtained using SSB telescope detectors. The solid squares are the present measurements and open squares are measurements by Mahata *et al.* [11]. Solid line is to guide the eyes.

Table 1. Deformation parameters (β_2, β_3), and excitation energies (E^*) of different states for different isotopes of Pt.

Nucleus	β_2	$E^*(2^+)$ (MeV)	β_3	$E^*(3^-)$ (MeV)
^{194}Pt	0.15	0.328	0.13	1.43
^{196}Pt	0.13	0.360	0.11	0.41
^{198}Pt	0.11	0.407	0.10	1.50

After fitting the experimental fusion cross-section the parameters are kept fixed and spin distributions are obtained for all the reactions at all energies. The CN spin distributions thus obtained are used as input for statistical model calculation. Figure 5 shows the comparison of the experiment and statistical model predicted fission cross-sections. It is observed that the statistical model prediction using shell corrected FRLDM barriers under-predicts the experimental fission cross-sections. This indicates the absence of dissipation effects. In order to explain the observed fission cross-sections the shell

corrected FRLDM barriers are lowered using a scaling factor (k_f) and the scaled barrier is given as

$$V_B(l, E^*) = k_f V_{LDM}(l) - \Delta V_{shl}(l)$$

where $V_{LDM}(l)$ is FRLDM barrier and $\Delta V_{shl}(l)$ is the shell correction in fission barrier. The statistical model calculations are carried out using k_f as a free parameter to fit the experimental fission cross-sections. It is observed that no single value of k_f is able to fit the experimental fission cross-sections at all the energies though an overall good fit is obtained at k_f = 0.80, 0.85and 0.75 for ^{217}Fr, ^{215}Fr and ^{213}Fr respectively.

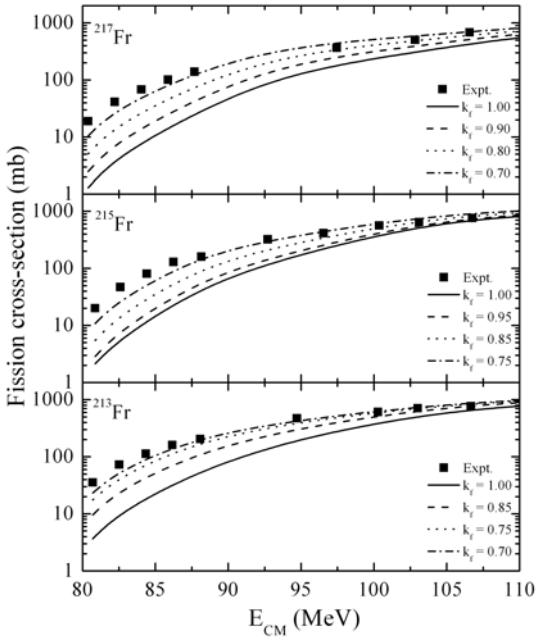

Figure 5. Experimental fission cross-section (filled squares) for different isotopes of Fr along with the statistical model calculation results for different values of scaling factor (k_f) using shell corrected FRLDM fission barriers.

5 Conclusions

The experimental fission excitation functions are measured for ^{217}Fr, ^{215}Fr and ^{213}Fr. Out of these ^{213}Fr is a shell closed CN and the other two nuclei are away from shell closure. It is observed that the fission cross-sections increase as one moves from ^{217}Fr to ^{213}Fr. This observation is in agreement with the trends as expected on the basis of fissilty parameter. This further indicates that shell closure in CN does not provide any extra stability against fission.

The measured fission cross-sections are compared with the statistical model predictions. It is observed that the model calculation with Bohr-Wheeler fission width and shell corrected FRLDM barrier under-predicts the experimental cross-sections. The fission barrier are reduced by introducing a scaling factor and an overall good fit of fission cross-sections is obtained using k_f = 0.80, 0.85 and 0.75 for ^{217}Fr, ^{215}Fr and ^{213}Fr respectively. This indicates that the nuclear dissipation is absent in pre-saddle region, though a considerable dissipation has been observed in the neutron multiplicity measurement [3]. Therefore, more theoretical studies with better modeling of fission are necessary and use of different dissipation strengths in the pre and post-saddle (shape dependent dissipation) dissipations may remove the apparent contradictions observed between the results from fission cross-sections and neutron multiplicity measurement analysis.

Acknowledgments

The financial support from the Council of Scientific and Industrial Research (CSIR), Government of India, in the form of a Shyama Prasad Mukherjee Research Grant (SPMF) to one of the authors (V.S.) is gratefully acknowledged.

References

1. D. Hilscher and H. Rossner, Ann. Phys. (Paris) **17**, 471 (1992).
2. M. Thoennessen and G. F. Bertsch, Phys. Rev. Lett. **71**, 4303 (1993).
3. Varinderjit Singh *et al.*, Phys. Rev. C **86**, 014609 (2012); Phys. Rev. C **87**, 064601 (2013).
4. Akhil Jhingan *et al.*, Proc. DAE-BRNS Symp. on Nucl. Phys. **56**, 1040 (2011).
5. V. E. Viola, K. Kwiatkowski and M. Walker, Phys. Rev. C **31**, 1550 (1985).
6. P. Frobrich and I. I. Gontchar, Phys. Rep. **292**, 131 (1998).
7. N. Bohr and J. A. Wheeler, Phys. Rev. **56**, 426 (1939).
8. A. V. Ignatyuk, M. G. Itkis, and S. I.Mulgin, Fiz. Elem. Chastits At. Yadra **16**, 709 (1985).
9. Y. Aritomo, Nucl. Phys. A **780**, 222 (2006).
10. J. Fernandez Niello, C.H. Dasso and S. Landowne, Comput. Phys. Commun. **54**, 409 (1989).
11. K. Mahata *et al.*, Phys. Rev. C **65**, 034613 (2002).
12. Varinderjit Singh *et al.*, Phys. Rev. C **89**, 024609 (2014).
13. S. Raman, C. W. Nestor and P. Tikkanen, Atomic Data and Nuclear Data Tables **78**, 1 (2001).
14. F. Todd Baker, Alan Scott, T. H. Kruse, W. Hartwig, E. Ventura, and W. Savin, Nucl. Phys. A **266**, 377 (1976).